

## Expression of the Mucosal Homing Receptor $\alpha_4\beta_7$ Correlates with the Ability of CD8<sup>+</sup> Memory T Cells To Clear Rotavirus Infection

JASON R. ROSÉ,<sup>1,2,3\*</sup> MARNA B. WILLIAMS,<sup>2,3,4\*</sup> LUSIJAH S. ROTT,<sup>2,3,4</sup> EUGENE C. BUTCHER,<sup>2,3,4</sup>  
AND HARRY B. GREENBERG<sup>1,2,3</sup>

*Departments of Medicine, Microbiology, and Immunology, Stanford University School of Medicine,<sup>1</sup> and Laboratory of Immunology and Vascular Biology, Department of Pathology,<sup>4</sup> and Digestive Disease Center,<sup>3</sup> Stanford University, Stanford, California 94305, and Veterans Affairs Palo Alto Health Care System, Palo Alto, California 94304<sup>2</sup>*

Received 18 March 1997/Accepted 16 October 1997

**The integrin  $\alpha_4\beta_7$  plays an important role in lymphocyte homing to mucosal lymphoid tissues and has been shown to define a subpopulation of memory T cells capable of homing to intestinal sites. Here we have used a well-characterized intestinal virus, murine rotavirus, to investigate whether memory/effector function for an intestinal pathogen is associated with  $\alpha_4\beta_7$  expression.  $\alpha_4\beta_7^{\text{hi}}$  memory phenotype (CD44<sup>hi</sup>),  $\alpha_4\beta_7^-$  memory phenotype, and presumptively naive (CD44<sup>lo</sup>) CD8<sup>+</sup> T lymphocytes from rotavirus-infected mice were sorted and transferred into Rag-2 (T- and B-cell-deficient) recipients that were chronically infected with murine rotavirus.  $\alpha_4\beta_7^{\text{hi}}$  memory phenotype CD8<sup>+</sup> cells were highly efficient at clearing rotavirus infection,  $\alpha_4\beta_7^-$  memory cells were inefficient or ineffective, depending on the cell numbers transferred, and CD44<sup>lo</sup> cells were completely unable to clear chronic rotavirus infection. These data demonstrate that functional memory for rotavirus resides primarily in memory phenotype cells that display the mucosal homing receptor  $\alpha_4\beta_7$ .**

Subsets of memory lymphocytes and immunoblasts display tissue-selective homing and recirculation (7, 9, 10, 19, 29, 37). These homing preferences are thought to reflect differential interaction of lymphocytes with specialized vascular endothelium mediated by differential expression of homing receptors on the surfaces of circulating memory/effector cells (6, 8, 9, 29, 37). The integrin  $\alpha_4\beta_7$ , for example, mediates lymphocyte recognition of the mucosal vascular addressin (MAdCAM-1) (4, 21) and is involved in lymphocyte homing to Peyer's patches (PP) and intestinal lamina propria (2, 4, 20, 31). Importantly, previously activated/memory T lymphocytes are subdivided into discrete  $\alpha_4\beta_7^{\text{hi}}$  and  $\alpha_4\beta_7^-$  populations (1, 13, 42) with distinctive patterns of MAdCAM-1 binding (39), recirculation (30), and homing (44). In particular, memory/effector cells expressing high levels of  $\alpha_4\beta_7$  home to intestinal PP and recirculate through intestinal tissues, whereas those that do not express  $\alpha_4\beta_7$  are virtually excluded. Such observations of differential  $\alpha_4\beta_7$  expression and homing properties of circulating memory T-cell subsets have led to the hypothesis that  $\alpha_4\beta_7^+$  memory cells may comprise cellular memory to mucosal antigens. However, this hypothesis has not been tested and the selective ability of such memory cells to exert a specific effector function at a mucosal surface has not been directly demonstrated.

Rotavirus is a segmented, double-stranded RNA virus of the family *Reoviridae* and is a major pathogen of the intestinal tract (15). Rotavirus infection occurs in, and is largely limited to, the villus enterocytes of the small intestine (18). The specificity of viral replication ensures that the immunologic response to rotavirus is focused in the intestinal compartment. In both neonatal and adult mice, large amounts of rotavirus-specific

immunoglobulin A (IgA) are found in stool samples following virus clearance and persist for up to 1 year following primary infection (5, 33). Virus-specific CD8<sup>+</sup> cytotoxic T lymphocytes (CTLs) are detected at the intestinal surface following acute infection (36), and passively transferred CTLs can both protect suckling mice against diarrhea (34) and migrate to the intestinal surface to clear chronic rotavirus infection in severe combined immunodeficiency mice (12) and Rag-2 mice (17). Rotavirus-specific CTLs are detected in mucosal nodes (PP and mesenteric lymph nodes [MLN]) early in infection and are later detected in the spleen, presumably after encountering rotavirus in the gut (35). Recently, we and others have shown that CD8<sup>+</sup> T cells play an important role in the timely resolution of primary rotavirus infection and a much lesser role in protection from reinfection (16, 17, 32, 34).

To test the hypothesis that expression of the mucosal integrin  $\alpha_4\beta_7$  might correlate with and function in defining memory for mucosa-restricted antigens, we sorted CD8<sup>+</sup> T-cell subsets from C57BL/6 mice which had previously been infected with murine rotavirus. The  $\alpha_4\beta_7^{\text{hi}}$  CD44<sup>hi</sup>,  $\alpha_4\beta_7^-$  CD44<sup>hi</sup>, and CD44<sup>lo</sup> subsets were transferred (separately) into Rag-2 (43) (T- and B-cell-deficient) recipients chronically infected with murine rotavirus, and viral clearance was monitored. We show that the  $\alpha_4\beta_7^{\text{hi}}$  CD44<sup>hi</sup> subset selectively clears rotavirus and that the ability to clear rotavirus is either rare or absent in the  $\alpha_4\beta_7^-$  CD44<sup>hi</sup> or presumptively naive (CD44<sup>lo</sup>) subsets of CD8<sup>+</sup> T cells. These results demonstrate for the first time that functional memory for a mucosal pathogen resides primarily in memory phenotype cells that display the mucosal homing receptor  $\alpha_4\beta_7$ .

### MATERIALS AND METHODS

**Mice, viruses, and viral inoculation.** Stocks of wild-type murine EC rotavirus were prepared as intestinal homogenates, and their titers were determined in mice as previously described (5). Stocks of tissue culture-adapted rhesus rotavirus (RRV) were prepared as previously described (22). Six-week-old C57BL/6 mice were obtained from the Charles River Laboratory (Hollister, Calif.) and bred in the Palo Alto Veteran's Administration breeding facility to be used as

\* Corresponding author. Mailing address: Department of Pathology, L235, Stanford University School of Medicine, Stanford, CA 94305-5487. Phone: (650) 493-5000, ext. 6-3122 (J. R. Rosé) or 6-3134 (M. B. Williams). Fax: (650) 852-3259 (J. R. Rosé) or (650) 858-3986 (M. B. Williams).

donors for cell transfer experiments. Prior to study, we showed by enzyme-linked immunosorbent assay (ELISA) that the serum of mice used in these experiments was negative for rotavirus antibody. Mice were orally gavaged with  $10^5$  50% diarrheal doses ( $DD_{50}$ ) of virus after receiving 100  $\mu$ l of 1.33% sodium bicarbonate to neutralize stomach acid. Viral shedding was monitored by ELISA to assess the progress of infection (5). One month following the initial infection, immunized mice were boosted by gavage with a second dose of virus ( $10^5$   $DD_{50}$ ). Splenocytes from donor mice were harvested for sorting experiments between 3 and 12 weeks after boosting. (Due to the extremely low number of rotavirus-responsive cells, we were unable to assay cytotoxicity *in vitro*; however, we inferred that there was no significant difference in cells harvested 3 versus 12 weeks after boosting, as we have shown that CD8<sup>+</sup> T cells can mediate partial long-term protection for up to 5 months after viral reinfection [17]. Also, shedding of rotavirus in  $J_HD^{-/-}$  mice challenged with rotavirus is the same 6 and 12 weeks after inoculation [32]. Recipient Rag-2 mice (43) were obtained from Taconic (Germantown, N.Y.) and infected with  $10^5$   $DD_{50}$  of the murine EC virus as previously described (16). Stool samples from infected mice were assayed for viral antigen at 2 weeks postinoculation to confirm the establishment of chronic infection. Rag-2 mice were chronically infected for 1 to 3 months prior to cell transfer.

**Detection of viral antigen.** Viral antigen detection was performed by ELISA as described previously (5). Briefly, microtiter plates (Dynatech, McLean, Va.) were coated with diluted hyperimmune guinea pig anti-RRV serum and blocked with 5% nonfat dry milk. Stool samples were made to a 10% suspension, added to plates, and incubated for 2 h at 37°C. Antigen was detected with rabbit anti-RRV serum, followed by horseradish peroxidase (HRP)-conjugated goat anti-rabbit serum (Kirkegaard & Perry Laboratories, Gaithersburg, Md.). Visualization was performed by incubation of plates with ABTS {2,2'-azino-di[3-ethylbenzthiazoline sulfonate (6)]} substrate (Kirkegaard & Perry), and then the reaction was quenched with 10% sodium dodecyl sulfate. Plates were read by using an EIA Autoreader (BIO-TEK Instruments, Burlington, Vt.) at 405 nm. Clearance was defined as the point at which ELISA values fell below an optical density (OD) of 0.08. To determine the background absorbance levels, stool samples from mice that had not been infected with rotavirus (OD,  $\leq 0.08$ ), in addition to wells with no stool sample (OD,  $\leq 0.04$ ), were assayed by ELISA. Also, samples were assayed in the absence of rabbit anti-RRV serum (OD,  $\leq 0.04$ ), in the absence of HRP-conjugated goat anti-rabbit serum (OD,  $\leq 0.05$ ), and in sample wells not coated with guinea pig anti-RRV serum (OD,  $-0.05$  to  $-0.06$ ).

Virus-specific antibodies were detected by first coating plates as described above and then incubating them overnight with a 1:5 dilution of RRV stock virus at 4°C. After three washes, 5% stool samples were added to the plates at 37°C. Antibody was detected with HRP-conjugated anti-mouse IgA or IgG (Kirkegaard & Perry) and visualized as described above. To determine background absorbance levels, stool samples from animals that were not infected with rotavirus were assayed (OD, 0.011 to 0.030;  $n = 6$ ).

**Antibodies and reagents.** For sorting, a biotinylated monoclonal antibody (MAB) to CD8 (Lyt2) and a phycoerythrin (PE)-conjugated MAB to  $\alpha_4\beta_7$  (DATK32) were purchased from PharMingen, La Jolla, Calif. A fluorescein isothiocyanate-conjugated MAB to CD44 (MJ64) (3) was produced and conjugated in the laboratory of E. C. Butcher. A biotinylated MAB to human CD44 (Hermes-1) (23), produced in the laboratory of E. C. Butcher, and PE-conjugated anti-rat-IgG2a (PharMingen) were used as isotype control antibodies. Streptavidin-Red 613 (Red 613) was purchased from GIBCO (Gaithersburg, Md.). Ascites containing antibodies against CD4 (GK1.4) and B220 (RA36B2), used for subtractive panning, was produced in the laboratory of E. C. Butcher.

**Staining and cell sorting.** Splenocytes to be sorted from donor rotavirus-infected C57BL/6 mice were harvested, disaggregated by teasing between glass slides, and pressed through stainless steel screen mesh (0.0021-in. diameter). Pooled cells were washed with 5 to 10 ml of Dulbecco's modified Eagle's medium supplemented with 10% fetal bovine serum (DMEM-10) and then treated with 5 ml of lysis buffer (0.15 M  $NH_4Cl$ , 1 mM  $KHCO_3$ , 0.1 mM  $Na_2EDTA$ ) for 5 min to lyse erythrocytes. After lysis, splenocytes were washed twice and resuspended in DMEM-10. The yield was typically  $1 \times 10^8$  to  $2 \times 10^8$  cells per harvested spleen. Splenocytes to be sorted were enriched for CD8<sup>+</sup> T cells by panning on plates coated with anti-CD4 and anti-B220 antibodies, as previously described (17). Panned cells were resuspended in DMEM-10.

Splenocytes ( $0.6 \times 10^7$  to  $1.2 \times 10^7$  cells/tube) were stained with MABs to CD8 (Lyt2; 0.5  $\mu$ g/ $10^6$  cells),  $\alpha_4\beta_7$  (DATK32; 0.09  $\mu$ g/ $10^6$  cells), and CD44 (MJ64; 1:150 dilution). Cells were incubated on ice for 20 min with MABs in 300  $\mu$ l of DMEM-10 and then washed at 4°C with 3 ml of DMEM-10. Splenocytes were then stained with Red 613 (0.5  $\mu$ l/ $10^6$  cells) for 20 min on ice, washed with 3 ml of DMEM-10, and resuspended in DMEM-10 for sorting.

Cells were sorted on a modified FACStar (Becton Dickinson, San Jose, Calif.) with a single 488-nm argon laser and three fluorescence detectors. Filters for the three fluorochromes were 530/30 for fluorescein isothiocyanate detection, 585/42 for PE detection, and 630/22 for Red 613 detection.

The  $\alpha_4\beta_7^-$  memory CD8<sup>+</sup> and naive CD8<sup>+</sup> populations were sorted twice to optimize purity. The level of purity after sorting once ( $98.7\% \pm 1.3\%$ ) was determined by using the FACStar. Because of the scarcity of cells, the purity of the transferred cells that had been sorted twice could not be determined; however, in parallel experiments, we determined by FACStar analysis that the purity after sorting twice was typically at least 99.7%. Double sorting of CD8<sup>+</sup> cells has

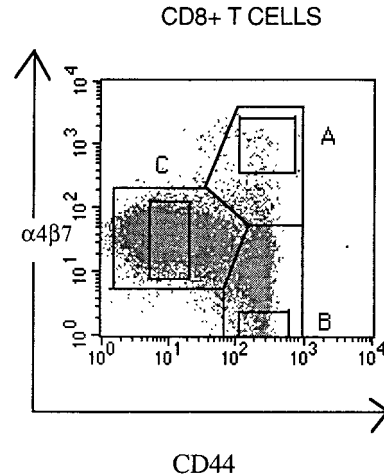


FIG. 1. CD8<sup>+</sup> splenic lymphocytes from rotavirus-immunized mice. Spleen cells were analyzed for the expression of  $\alpha_4\beta_7$  and CD44 by flow cytometry after subtractive panning of B220<sup>+</sup> and CD4<sup>+</sup> T cells. The FACS dot plot shows three distinct populations (delineated on the plot) of CD8<sup>+</sup> gated small lymphocytes: one naive-phenotype (CD44<sup>lo</sup>) and two memory phenotype ( $\alpha_4\beta_7^hi$  CD44<sup>hi</sup> and  $\alpha_4\beta_7^-$  CD44<sup>hi</sup>) populations. Typical gates used to sort  $\alpha_4\beta_7^hi$  CD44<sup>hi</sup> (A),  $\alpha_4\beta_7^-$  CD44<sup>hi</sup> (B), and naive-phenotype (C) cells are shown on the plot.

no effect on the efficiency of CD8<sup>+</sup> T-cell-mediated rotavirus clearance (17). Approximately 20,000  $\alpha_4\beta_7^hi$  CD44<sup>hi</sup> (single-sorted) and  $\alpha_4\beta_7^-$  CD44<sup>hi</sup> (double-sorted) cells were obtained from an input of  $7 \times 10^7$  panned (depleted of B220<sup>+</sup> and CD4<sup>+</sup> cells) splenocytes. Sorted donor cells were resuspended in sterile saline solution at  $10^5$ /ml and injected intraperitoneally into chronically infected Rag-2 mice.

## RESULTS

**Splenic CD8<sup>+</sup> lymphocytes can be partitioned into three distinct populations.** Figure 1 shows a representative fluorescence-activated cell sorter (FACS) plot of gated small CD8<sup>+</sup> splenocytes from rotavirus-immunized mice. Cells were stained with MABs to CD44 and the mucosal homing receptor  $\alpha_4\beta_7$ . We used CD44 as a marker for memory/effector T cells, as an increase in CD44 expression correlates with memory/effector function in certain strains of mice, including C57BL/6 (14, 28). We selectively analyzed small lymphocytes (as opposed to blasts) by gating on cells with decreased forward scatter intensity (compared to the higher intrinsic forward scatter of blasts). Three distinct populations can be identified in the plot:  $\alpha_4\beta_7^hi$  memory (CD44<sup>hi</sup>),  $\alpha_4\beta_7^-$  memory (CD44<sup>hi</sup>), and  $\alpha_4\beta_7^{lo}$  naive (CD44<sup>lo</sup> to CD44<sup>-</sup>). No significant differences were observed in staining patterns between naive mice and mice immunized with rotavirus (data not shown), and the subsets identified in Fig. 1 represent 4% ( $\alpha_4\beta_7^hi$  memory phenotype), 28% ( $\alpha_4\beta_7^-$  memory phenotype), and 66% (naive) of the total CD8<sup>+</sup> population. Sort gates were established to select the brightest of the  $\alpha_4\beta_7^hi$  memory phenotype cells (2% of the total CD8<sup>+</sup> cells), the most weakly staining  $\alpha_4\beta_7^-$  memory phenotype cells (6% of the total CD8<sup>+</sup> cells), and naive-phenotype cells comprising the population staining at low levels for CD44 (30% of the total CD8<sup>+</sup> cells) (Fig. 1). We sorted cells from the spleen, an organ that efficiently recruits both  $\alpha_4\beta_7^hi$  and  $\alpha_4\beta_7^-$  memory cells from the blood (44), to obtain significant numbers of all three populations.

**CD8<sup>+</sup> T cells expressing high levels of  $\alpha_4\beta_7$  and CD44 clear rotavirus infection.** Splenocytes were stained with CD44 to identify previously activated (presumptive memory) lymphocytes (14, 28) among the  $\alpha_4\beta_7^hi$  and  $\alpha_4\beta_7^-$  cells. When 20,000  $\alpha_4\beta_7^hi$  memory cells (CD44<sup>hi</sup>) were transferred into recipients,

TABLE 1. Effect of cell surface phenotype and number of cells transferred on rate of rotavirus clearance

Phenotype sorted by FACS (no. of mice)	No. of cells transferred	Day(s) virus cleared posttransfer
$\alpha_4\beta_7^{\text{hi}}$ CD8 <sup>+</sup> CD44 <sup>hi</sup> (3)	20,000	4, 4, 5
$\alpha_4\beta_7^-$ CD8 <sup>+</sup> CD44 <sup>hi</sup> (3)	20,000	16, 16, 16
CD8 <sup>+</sup> CD44 <sup>lo</sup> (3)	20,000	>90
$\alpha_4\beta_7^{\text{hi}}$ CD8 <sup>+</sup> CD44 <sup>hi</sup> (5)	10,000	16 ± 0.5 <sup>a</sup>
$\alpha_4\beta_7^-$ CD8 <sup>+</sup> CD44 <sup>hi</sup> (6)	10,000	>60 <sup>b</sup>
CD8 <sup>+</sup> CD44 <sup>lo</sup> (5)	10,000	>60 <sup>b</sup>

<sup>a</sup> Represents the mean ± standard deviation of results pooled from two experiments, one with two recipients and one with three.

<sup>b</sup> Represents the terminal day when rotavirus antigen was assayed in stool samples. Results are either from three experiments, each with two recipients ( $\alpha_4\beta_7^-$ CD8<sup>+</sup>CD44<sup>hi</sup>), or from two experiments, one with three recipients and one with two recipients (CD8<sup>+</sup>CD44<sup>lo</sup>). No clearance was seen in any mouse receiving these subsets.

viral clearance occurred in 4 to 5 days (Table 1). Naive (CD44<sup>lo</sup>) CD8<sup>+</sup> cells derived from rotavirus-immunized mice were unable to clear the virus. Antigen shedding in recipients of naive CD8<sup>+</sup> cells continued for up to 3 months, when the experiment was terminated. When 20,000  $\alpha_4\beta_7^-$  CD44<sup>hi</sup> cells were transferred, mice cleared the virus, although only after a substantial delay (16 days; 11 to 12 days longer than  $\alpha_4\beta_7^{\text{hi}}$  cells) (Table 1).

We speculated that clearance in mice receiving  $\alpha_4\beta_7^-$  cells could be due to small numbers of  $\alpha_4\beta_7^{\text{hi}}$  cells which were not removed during the sorting ( $\geq 99.7\%$  purity). These cells could undergo proliferation and expansion after transfer, thereby clearing the virus after an initial lag phase. We reasoned that transfer of limiting numbers of cells should reduce or eliminate the lymphocytes capable of clearing virus from the  $\alpha_4\beta_7^-$ -treated mice. To test this hypothesis, we conducted a series of experiments in which 10,000 cells of each phenotype were transferred. When 10,000 sorted cells were transferred, neither mice receiving CD44<sup>lo</sup> cells nor mice receiving  $\alpha_4\beta_7^-$  CD44<sup>hi</sup> cells were able to clear the virus, even 60 days after cell transfer (when the experiment was terminated) (Table 1; Fig. 2). In contrast, all mice receiving 10,000  $\alpha_4\beta_7^{\text{hi}}$  CD44<sup>hi</sup> CD8<sup>+</sup> cells cleared the virus within 16 to 17 days.

## DISCUSSION

Our results indicate dramatic differences between the abilities of naive,  $\alpha_4\beta_7^{\text{hi}}$  memory, and  $\alpha_4\beta_7^-$  memory CD8<sup>+</sup> spleen cells to clear chronic rotavirus infection after passive transfer. Only the populations of CD8<sup>+</sup> cells expressing high levels of the  $\alpha_4\beta_7$  integrin and the CD44 memory marker were able to clear rotavirus in limiting-dilution assays. Naive (CD44<sup>lo</sup>) CD8<sup>+</sup> cells were unable to clear the virus after transfer into infected Rag-2 mice, an observation consistent with the reported requirement for CD4<sup>+</sup> T-cell help during primary CTL responses to some rotaviral infections (16a). Elimination of rotavirus by  $\alpha_4\beta_7^-$  cells was significantly delayed at all cell doses and was observed only when 20,000 cells were transferred.

The kinetics of clearance by transferred memory cells was dependent on cell number, as demonstrated by the difference between the clearance rates obtained by using different protocols (Table 1), as well as CD44 expression ( $n = 2$ ; data not shown). Transfer of 20,000  $\alpha_4\beta_7^{\text{hi}}$  CD44<sup>hi</sup> cells resulted in significantly faster clearance than transfer of 10,000  $\alpha_4\beta_7^{\text{hi}}$  CD44<sup>hi</sup> cells. The delay in clearance following transfer of lim-

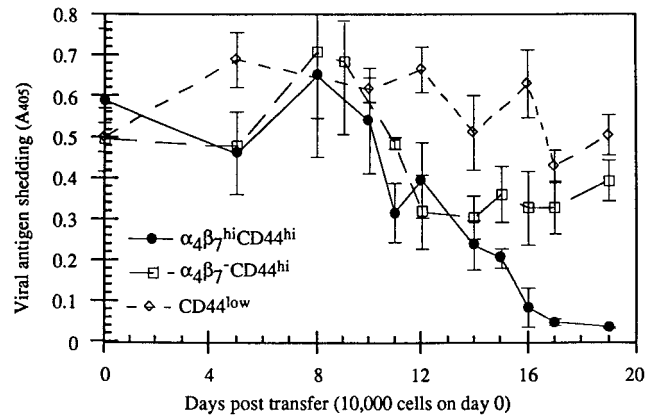


FIG. 2. Viral antigen shedding in Rag-2 mice chronically infected with murine rotavirus after passive transfer of CD8<sup>+</sup> T cells. Ten thousand sorted lymphocytes from immunized C57BL/6 donor mice were resuspended in sterile saline and injected intraperitoneally into chronically infected recipient Rag-2 mice. Viral shedding was monitored by ELISA of stool samples (see Materials and Methods). OD values were considered significant if they exceeded 0.08, which was the lower limit of detection by ELISA. Error bars represent the standard deviation of data acquired from results pooled from two or three experiments with five or six mice (as described in Table 1). The reduction in viral shedding between 12 and 17 days after transfer of  $\alpha_4\beta_7^-$  CD44<sup>hi</sup> cells was not statistically significant, as we have often observed similar variations in rotavirus levels in infected Rag-2 mice that did not receive sorted cells (OD values: day 0, 0.575; day 7, 0.297; day 13, 0.355; day 40, 0.543).

iting cell numbers may be attributed to the expansion of a small number of rotavirus-specific T cells to a population size adequate for elimination of the virus.

$\alpha_4\beta_7^-$  cells were unable to clear the virus even at later time points when transferred at 10,000 cells/recipient. Although we cannot formally exclude the possibility of the existence of  $\alpha_4\beta_7^-$  rotavirus-specific CD8<sup>+</sup> cells (whose efficiency in clearing virus might be compromised by inefficient access to the mucosal lamina propria—see below) in these *in vivo* studies, the complete inability of 10,000  $\alpha_4\beta_7^-$  CD8<sup>+</sup> cells to eliminate the virus even after 60 days demonstrates that functional memory for this intestinal viral pathogen is comprised of  $\alpha_4\beta_7^{\text{hi}}$  cells and suggests that this inability reflects segregation of rotavirus-specific CD8<sup>+</sup> effector cells into the  $\alpha_4\beta_7^{\text{hi}}$  subset during the intestinal immune response.

While it appears that effective memory for rotavirus resides primarily among  $\alpha_4\beta_7^{\text{hi}}$  CD44<sup>hi</sup> CD8<sup>+</sup> cells, rotavirus-specific cells may not be exclusively in this subset. Transfer of 20,000  $\alpha_4\beta_7^-$  CD44<sup>hi</sup> CD8<sup>+</sup> cells resulted in clearance, although with much slower kinetics than clearance by  $\alpha_4\beta_7^{\text{hi}}$  CD44<sup>hi</sup> CD8<sup>+</sup> cells. Delayed clearance by the  $\alpha_4\beta_7^-$  population could be due in part to inefficient access to the mucosa in the absence of this intestinal homing receptor. In this scenario,  $\alpha_4\beta_7^-$  effector cells might acquire  $\alpha_4\beta_7$  after transfer, thus explaining the delay in clearance. The malleability of homing receptor expression has not been established, but in parallel preliminary experiments in which double-sorted  $\alpha_4\beta_7^-$  CD44<sup>hi</sup> CD8<sup>+</sup> cells were transferred into Rag-2 mice chronically infected with rotavirus, we observed a low but significant percentage of  $\alpha_4\beta_7^{\text{hi}}$  cells (~3 to 10% of gated CD8<sup>+</sup> small lymphocytes) in the spleens and MLN of animals that had cleared the virus, with slightly fewer (~2 to 5%) in animals which had not cleared the virus. On the other hand, as discussed above, clearance by the sorted  $\alpha_4\beta_7^-$  population may be due to a small percentage of contaminating  $\alpha_4\beta_7^{\text{hi}}$  cells (estimated as <0.03%), which are unavoidable during the sorting procedure.

Infection of mice with viruses which replicate in mucosal



tissues leads to an immune response that is targeted to mucosal sites. Studies of the development of the immune response to rotavirus have shown the rapid appearance of virus-specific CTLs in the PP and MLN after infection (36). Likewise, infection with reovirus, another mucosa-specific virus, leads to an enrichment of virus-reactive CTLs in the intestinal intraepithelial lymphocytes and PP (11, 16, 17, 25, 26), as well as an increase in the frequency of virus-specific B cells and CD4<sup>+</sup> T cells in PP as opposed to peripheral lymph nodes (27). The enrichment of virus-reactive cells in mucosal versus nonmucosal compartments suggests a mechanism by which these cells are directed to mucosal compartments.

Previous and concurrent studies have examined the segregation of memory for regional immune responses into homing receptor-defined subsets of CD4<sup>+</sup> cells or of antibody-producing B effector or effector precursor cells. In studies of human CD4<sup>+</sup> proliferative responses, for example, we have found that rotavirus-specific memory following natural infection segregates selectively to the  $\alpha_4\beta_7^{\text{hi}}$  CD4<sup>+</sup> cells, whereas proliferative CD4<sup>+</sup> cells responding to intramuscular mumps vaccine are largely  $\alpha_4\beta_7^-$  (40). Human CD4<sup>+</sup> T cells responsive to nickel and dust mite cutaneous antigens involved in allergic dermatitis are enriched among cells displaying the cutaneous lymphocyte antigen skin-homing receptor (41), a population that, in contrast to intestinal rotavirus-reactive cells, lacks the mucosal homing receptor  $\alpha_4\beta_7$  (39). Furthermore, a humoral, as well as a CD8-mediated, cellular immune response can also clear chronic rotavirus infection in the immunodeficient mouse model, and ongoing studies have revealed compartmentalization of rotavirus-specific B-cell responses, with the  $\alpha_4\beta_7^{\text{hi}}$  memory phenotype subset selectively clearing the virus and secreting rotavirus-specific, stool-localized IgA (43a). Finally, our findings here are consistent with recent studies of antigen-specific antibody-secreting cells induced by gastrointestinal versus systemic immunization with defined antigens, which resulted in enrichment or depletion of  $\alpha_4\beta_7$  expression, respectively (23, 24, 38). The expression of  $\alpha_4\beta_7$  by functional immune cells for mucosal pathogens may have important implications for vaccine development and suggests that the efficiency of generation of  $\alpha_4\beta_7^+$  (versus  $\alpha_4\beta_7^-$ ) memory may correlate with functional gastrointestinal immunity.

In conclusion, our findings confirm that memory CD8<sup>+</sup> cells, like their CD4<sup>+</sup> counterparts, can be subdivided based on differential homing receptor expression (13, 39), demonstrate that functional memory for rotavirus resides primarily in memory phenotype cells that display the mucosal homing receptor  $\alpha_4\beta_7$ , and support the importance of differential homing receptor expression in the compartmentalization of immune responses.

#### ACKNOWLEDGMENTS

J. R. Rosé and M. B. Williams contributed equally to this report, and H. B. Greenberg and E. C. Butcher contributed equally as senior authors.

This research was supported by Microbiology and Immunology training grant 5T32AI07328-09 (J.R.R.), NIH National Research Service Award AI08872 from the National Institute of Allergy and Infectious Diseases (M.B.W.), the FACS Core Facility of the Stanford Digestive Disease Center under grant DK38707 (L.S.R.), NIH grant AI37832 (E.C.B.), NIH grant R37 AI21362 (H.B.G.), and V. A. Medical Investigator Awards from the Department of Veterans Affairs Palo Alto Health Care System (E.C.B. and H.B.G.).

We thank members of the Butcher and Greenberg laboratories for illuminating discussions, especially M. Franco.

#### REFERENCES

1. Andrew, D. P., L. S. Rott, P. J. Kilshaw, and E. C. Butcher. 1996. Distribution of  $\alpha_4\beta_7$  and  $\alpha_E\beta_7$  on thymocytes, intestinal epithelial lymphocytes, and

- peripheral lymphocytes. *Eur. J. Immunol.* **26**:897–905.
2. Bargatze, R. F., M. A. Jutila, and E. C. Butcher. 1995. Distinct roles of L-selectin and integrins  $\alpha_4\beta_7$  and LFA-1 in lymphocyte homing to Peyer's patch-HEV *in situ*: the multistep model confirmed and refined. *Immunity* **3**:99–108.
3. Berg, E. L., M. K. Robinson, R. A. Warnock, and E. C. Butcher. 1991. The human peripheral lymph node vascular addressin is a ligand for LECAM-1, the peripheral lymph node homing receptor. *J. Cell Biol.* **114**:343–349.
4. Berlin, C., E. L. Berg, M. J. Briskin, D. P. Andrew, P. J. Kilshaw, B. Holzmann, I. L. Weissman, A. Hamann, and E. C. Butcher. 1993.  $\alpha_4\beta_7$  integrin mediates lymphocyte binding to the mucosal vascular addressin MAdCAM-1. *Cell* **74**:185–195.
5. Burns, J. W., A. A. Krishnaney, P. T. Vo, R. V. Rouse, L. J. Anderson, and H. B. Greenberg. 1995. Analysis of homologous rotavirus infection in the mouse model. *Virology* **207**:143–153.
6. Butcher, E., and W. Ford. 1986. Following cellular traffic: methods of labeling lymphocytes and other cells to trace their migration *in vivo*. In D. Weir and L. A. Herzenberg (ed.), *Handbook of experimental immunology*, 4th ed. Blackwell Scientific Publishers, Palo Alto, Calif.
7. Butcher, E. C. 1986. The regulation of lymphocyte traffic. *Curr. Top. Microbiol. Immunol.* **128**:85–122.
8. Butcher, E. C., and L. J. Picker. 1996. Lymphocyte homing and homeostasis. *Science* **272**:60–66.
9. Butcher, E. C., R. G. Scollay, and I. L. Weissman. 1980. Organ specificity of lymphocyte migration: mediation by highly selective lymphocyte interactions with organ-specific determinants on high endothelial venules. *Eur. J. Immunol.* **10**:556–561.
10. Cahill, R. N. P., D. C. Poskitt, H. Frost, and Z. Trnka. 1977. Two distinct pools of recirculating T lymphocytes: migratory characteristics of nodal and intestinal T lymphocytes. *J. Exp. Med.* **145**:420–428.
11. Cuff, C. E., C. K. Cebra, D. H. Rubin, and J. J. Cebra. 1993. Developmental relationship between cytotoxic a/b receptor-positive intraepithelial lymphocytes and Peyer's patch lymphocytes. *Eur. J. Immunol.* **23**:12333–12339.
12. Dharakul, T., L. Rott, and H. B. Greenberg. 1990. Recovery from chronic rotavirus infection in mice with severe combined immunodeficiency: virus clearance mediated by adoptive transfer of immune CD8<sup>+</sup> lymphocytes. *J. Virol.* **64**:4375–4382.
13. Erle, D. J., M. J. Briskin, E. C. Butcher, A. Garcia-Pardo, A. I. Lazarovits, and M. Tidswell. 1994. Expression and function of the MAdCAM-1 receptor, integrin  $\alpha_4\beta_7$ , on human leukocytes. *J. Immunol.* **153**:517–528.
14. Ernst, D. N., W. O. Weigle, D. J. Noonan, D. N. McQuitty, and M. V. Hobbs. 1993. The age-associated increase in IFN-gamma synthesis by mouse CD8<sup>+</sup> T cells correlates with shifts in the frequencies of cell subsets defined by membrane CD44, CD45R<sub>b</sub>, 3G11, and MEL-14 expression. *J. Immunol.* **151**:575–587.
15. Estes, M. K. 1996. Rotaviruses and their replication, p. 1625–1655. In B. N. Fields, D. M. Knipe, and P. M. Howley (ed.), *Fields virology*, 3rd ed., vol. 2. Lippincott-Raven Publishers, Philadelphia, Pa.
16. Franco, M. A., and H. B. Greenberg. 1995. Role of B cells and cytotoxic T lymphocytes in rotavirus infection. *J. Virol.* **69**:7800–7806.
- 16a. Franco, M. A., and H. B. Greenberg. Unpublished data.
17. Franco, M. A., C. Tin, L. S. Rott, J. L. VanCott, J. R. McGhee, and H. B. Greenberg. 1997. Evidence for CD8<sup>+</sup> T-cell immunity to murine rotavirus in the absence of perforin, Fas, and gamma interferon. *J. Virol.* **71**:479–486.
18. Greenberg, H. B., H. F. Clark, and P. A. Offit. 1994. Rotavirus pathology and pathophysiology, p. 255–283. In R. F. Ramig (ed.), *Rotaviruses*, vol. 185. Springer-Verlag KG, Berlin, Germany.
19. Guy-Grand, D., C. Griscelli, and P. Vassalli. 1974. The gut-associated lymphoid system: nature and properties of the large dividing cells. *Eur. J. Immunol.* **4**:435–443.
20. Hamann, A., D. P. Andrew, D. Jablonski-Westrich, B. Holzmann, and E. C. Butcher. 1994. Role of  $\alpha_4$ -integrins in lymphocyte homing to mucosal tissues *in vivo*. *J. Immunol.* **152**:3282–3293.
21. Holzmann, B., B. W. McIntyre, and I. L. Weissman. 1989. Identification of a murine Peyer's patch-specific lymphocyte homing receptor as an integrin molecule with an  $\alpha$  chain homologous to human VLA-4 $\alpha$ . *Cell* **56**:37–46.
22. Hoshino, Y., R. G. Wyatt, H. B. Greenberg, J. Flores, and A. Z. Kapikian. 1984. Serotypic similarity and diversity of rotaviruses of mammalian and avian origin as studied by plaque reduction neutralization. *J. Infect. Dis.* **149**:694–702.
23. Jalkanen, S. T., R. F. Bargatze, L. R. Herron, and E. C. Butcher. 1986. A lymphoid cell surface glycoprotein involved in endothelial cell recognition and lymphocyte homing in man. *Eur. J. Immunol.* **16**:1195–1202.
24. Kantele, J. M., H. Arvilommi, S. Kontiainen, M. Salmi, S. Jalkanen, E. Savilahti, M. Westerholm, and A. Kantele. 1996. Mucosally activated circulating human B cells in diarrhea express homing receptors directing them back to the gut. *Gastroenterology* **110**:1061–1067.
25. London, S. D., J. J. Cebra, and D. H. Rubin. 1989. Intraepithelial lymphocytes contain virus-specific, MHC-restricted cytotoxic cell precursors after gut mucosal immunization with reovirus serotype 1/Lang. *Reg. Immunol.* **2**:98–102.
26. London, S. D., J. A. Cebra-Thomas, D. H. Rubin, and J. J. Cebra. 1990. CD8

- lymphocyte subpopulations in Peyer's patches induced by reovirus serotype 1 infection. *J. Immunol.* **144**:3187–3194.
27. **London, S. D., D. H. Rubin, and J. J. Cebra.** 1987. Gut mucosal immunization with reovirus serotype 1/L stimulates virus-specific cytotoxic T cell precursors as well as IgA memory cells in Peyer's patches. *J. Exp. Med.* **165**: 830–847.
  28. **MacDonald, H. R., R. C. Budd, and J.-C. Cerottini.** 1990. Pgp-1 (Ly 24) as a marker of murine memory T lymphocytes. *Curr. Top. Microbiol. Immunol.* **159**:97–109.
  29. **Mackay, C. R.** 1993. Immunological memory. *Adv. Immunol.* **53**:217–265.
  30. **Mackay, C. R., D. P. Andrew, M. Briskin, D. J. Ringler, and E. C. Butcher.** 1996. Phenotype and migration properties of three major subsets of tissue-homing T cells in sheep. *Eur. J. Immunol.* **26**:1892–1898.
  31. **Mackay, C. R., W. L. Marston, L. Dudler, O. Spertini, T. F. Tedder, and W. R. Hein.** 1992. Tissue-specific migration pathways by phenotypically distinct subpopulations of memory T cells. *Eur. J. Immunol.* **22**:887–895.
  32. **McNeal, M. M., K. S. Barone, M. N. Rae, and R. L. Ward.** 1995. Effector functions of antibody and CD8<sup>+</sup> cells in resolution of rotavirus infection and protection against reinfection in mice. *Virology* **214**:387–397.
  33. **McNeal, M. M., and R. L. Ward.** 1995. Long-term production of rotavirus antibody and protection against reinfection following a single infection of neonatal mice with murine rotavirus. *Virology* **211**:474–480.
  34. **Offit, P., and K. I. Dudzik.** 1990. Rotavirus-specific cytotoxic T lymphocytes passively protect against gastroenteritis in suckling mice. *J. Virol.* **64**:6325–6328.
  35. **Offit, P. A., S. L. Cunningham, and K. I. Dudzik.** 1991. Memory and distribution of virus-specific cytotoxic T lymphocytes (CTLs) and CTL precursors after rotavirus infection. *J. Virol.* **65**:1318–1324.
  36. **Offit, P. A., and K. I. Dudzik.** 1989. Rotavirus-specific cytotoxic T lymphocytes appear at the intestinal mucosal surface after rotavirus infection. *J. Virol.* **63**:3507–3512.
  37. **Picker, L. J., and E. C. Butcher.** 1992. Physiological and molecular mechanisms of lymphocyte homing. *Annu. Rev. Immunol.* **10**:561–591.
  38. **Quiding-Jarbrink, M., I. Nordstrom, G. Granstrom, A. Kilander, M. Jertborn, E. C. Butcher, A. I. Lazarovits, J. Holmgren, and C. Czerkinsky.** 1997. Differential expression of tissue-specific adhesion molecules on human circulating antibody-forming cells after systemic, enteric, and nasal immunizations: a molecular basis for the compartmentalization of effector B cell responses. *J. Clin. Invest.* **99**:1281–1286.
  39. **Rott, L. S., M. J. Briskin, D. P. Andrew, E. L. Berg, and E. C. Butcher.** 1996. A fundamental subdivision of circulating lymphocytes defined by adhesion to mucosal addressin cell adhesion molecule-1. *J. Immunol.* **156**:3727–3736.
  40. **Rott, L. S., J. R. Rose, D. Bass, M. B. Williams, H. B. Greenberg, and E. C. Butcher.** 1997. Expression of mucosal homing receptor  $\alpha 4\beta 7$  by circulating CD4<sup>+</sup> cells with memory for intestinal rotavirus. *J. Clin. Invest.* **100**:1204–1208.
  41. **Santamaria Babi, L. F., L. J. Picker, M. T. Perez Soler, K. Drzimalla, P. Flohr, K. Blaser, and C. Hauser.** 1995. Circulating allergen-reactive T cells from patients with atopic dermatitis and allergic contact dermatitis express the skin-selective homing receptor, the cutaneous lymphocyte-associated antigen. *J. Exp. Med.* **181**:1935–1940.
  42. **Schweighoffer, T., Y. Tanaka, M. Tidswell, D. J. Erlse, G. E. Luce, A. I. Lazarovits, D. Buck, and S. Shaw.** 1993. Selective expression of  $\alpha 4\beta 7$  integrin on a subset of CD4<sup>+</sup> memory T cells with hallmarks of gut tropism. *J. Immunol.* **151**:717–729.
  43. **Shinkai, Y., G. Rathbun, K.-P. Lam, E. M. Oltz, V. Stewart, M. Mendelsohn, J. Charron, M. Datta, F. Young, A. M. Stall, and F. W. Alt.** 1992. RAG-2 deficient mice lack mature lymphocytes owing to inability to initiate V(D)J rearrangement. *Cell* **68**:855–867.
  - 43a. **Williams, M., et al.** Unpublished data.
  44. **Williams, M. B., and E. C. Butcher.** 1997. Homing of naive and memory T lymphocyte subsets to Peyer's patches, lymph nodes, and spleen. *J. Immunol.* **159**:1746–1752.